https://doi.org/10.3311/PPci.15586

Periodica Polytechnica Civil Engineering

Three-dimensional FSI Simulation by Using a Novel Hybrid Scaling – Application to the Tacoma Narrows Bridge

Gergely Szabó[1*], József Györgyi[2], Gergely Kristóf[3]

[1] Pont-TERV Ltd. Engineering Consultants, H-1119 Budapest, Than Károly u. 3-5, Hungary
[2] Department of Structural Mechanics, Faculty of Civil Engineering, Budapest University of Technology and Economics, H-1521 Budapest, P.O.B. 91, Hungary
[3] Department of Fluid Mechanics, Faculty of Mechanical Engineering, Budapest University of Technology and Economics, H-1521 Budapest, P.O.B. 91, Hungary
[*] Corresponding author, e-mail: drszabo@pontterv.hu

Received: 16 January 2020, Accepted: 02 June 2020, Published online: 27 July 2020

Abstract

In this paper a novel fluid-structure interaction approach for simulating flutter phenomenon is presented. The method is capable of modelling the structural motion and the fluid flow coupling in a fully three-dimensional manner. The key step of the proposed FSI procedure is a hybrid scaling of the physical fields; certain properties of the CFD simulation are scaled, while those of the mechanical system are kept original. This kind of scaling provides a significant speedup, since the number of the costly CFD time steps can be remarkably reduced. The acceptable computational time makes it possible to consider complex engineering problems such as buffeting, vortex shedding or flutter of a bridge deck or a wing of an airplane.

Keywords

torsional instability, fluid-structure interaction (FSI), aero-elasticity, modal analysis, hybrid scaling

1 Introduction

In the past decades really slender bridges have been built. Wind sensitivity of such buildings are well known, therefore their thorough dynamic calculation due to wind loading is essential. In the early ages of bridge aerodynamics, wind tunnel tests were used. Since the collapse of the Tacoma Narrows Bridge, a series of experimental tests were performed in order to unveil the reasons [1–2]. Billah and Scanlan [3] concluded these findings. These measurements were based on basically section wind tunnel models. Later on, with the strong need to capture the complex three-dimensional mutual interaction of the structural oscillation and the airflow around it, more sophisticated full aero-elastic wind tunnel models were applied. In the case of a number of large span bridges, these advanced tests were used [4–7]. Both the section and full aero-elastic models have their advantages and disadvantages. The full aero-elastic model approach is preferred for its capability to consider the whole bridge structure and the dynamic mode shapes as well as the corresponding natural frequencies and modal damping. These parameters need special care to adjust accurately, therefore the aero-elastic wind tunnel testing is rather costly. As the whole bridge structure is to be placed into the wind tunnel, the scaling needs to be higher (1:100~1:300) compared to the section models (1:20~1:60), leading to miniature ancillaries (e.g. fairings), and limited Reynolds-number achieved. Therefore, as to accuracy of aerodynamics, the more detailed section models can be expected to provide better results.

In the past several years, Computational Fluid Dynamics (CFD) has become popular in bridge aerodynamics. The wind tunnel tests can apparently be guided or even be replaced by numerical modelling. A series of successful numerical section studies have been performed with detailed validation to measurements [8–11]. A full review of these is found in [12]. These CFD simulations can be applied either to coupled fluid-structure interaction simulations, or to the flutter derivatives theory by means of forced oscillation method. By using CFD, the geometry scaling is not necessary contrary to the wind tunnel tests, which is the greatest advantage of the CFD. The prototype bridge geometry and wind speed can be considered, therefore the real Reynolds-number is ensured.

Cite this article as: Szabó, G., Györgyi, J., Kristóf, G. "Three-dimensional FSI Simulation by Using a Novel Hybrid Scaling – Application to the Tacoma Narrows Bridge", Periodica Polytechnica Civil Engineering, 2020. https://doi.org/10.3311/PPci.15586

Despite the fact that a number of commercial software offer convenient coupled fluid-structure interaction solutions, a validated fully aero-elastic fluid-structure interaction (FSI) simulation of a bridge deck is rare in literature [13]. Instead, the structure is modelled in a three-dimensional manner, the flow field is considered two dimensional [14–15]. The authors have invested a lot in order to exploit the advantages of CFD so as to perform coupled simulations. As a first step, a full aero-elastic wind tunnel model was constructed for validation purposes by Szabo et al. [16]. The critical wind speed of coupled flutter was well captured by using an FSI simulation, in which the FLUENT [17] commercial software was utilized. The aerodynamic forces were calculated via the software, while the structural dynamic motion of the bridge deck as well as the deformation of the CFD cells were handled by user defined functions (UDFs). With the application of the dynamic mode shapes and natural frequencies of the mechanical model, and using a simple explicit coupling technique, the simulation can be acceptably fast. Although this study was an idealized simulation case, provided promising results and offered an FSI approach that seemed capable of handling real bridge projects.

In order to further develop our FSI technique, it was deployed for commercial projects as well by Szabó et al. [18]. The conclusion was that the FSI simulation in case of a real bridge structure with high Reynolds-number needed significantly higher computational time, due to two reasons. First of all, the high Reynolds-number requires finer mesh near the bridge deck boundary in order to meet the y+=30~300 criteria for a high Reynolds-number turbulence model, consequently the CFD model contains more cells. Smaller cells call for smaller CFD time steps in order to keep Courant-Freud-Levy (CFL) number below 1 [19]. Secondly, the real bridge has lower natural frequencies than a wind tunnel model (higher periods of oscillation), therefore the flutter motion calculation needs more time to capture. These two reasons may provide explanation for the rare application of full aero-elastic FSI in bridge and building aerodynamics.

When scrutinizing the literature of aircraft aerodynamics, however, the case is different; a number of full aero-elastic FSI simulation can already be found that consider a whole airplane with the body and the wings altogether in a complex model. A complete F-16 jet fighter model was included in an FSI by Farhat et al. [20], for instance. There are reasons for the popularity of full aero-elastic FSI in the field of aircraft aerodynamics. The airplanes are streamlined in nature; no massive flow separation happens in case of a flutter phenomenon, therefore larger boundary layer cells can be enough in the CFD model. The larger the size of the cells, the larger the maximum CFD time steps can be allowed. Still, a complex three-dimensional approach is indeed time-consuming even in case of aircraft modelling. It seems obvious to use a large number of processors that can handle tremendous amounts of CFD cells. When a PC with limited resources (processor, RAM) is available only, that is commonly the case at a design office for instance, special considerations need to be made during the model creation in order to vastly reduce the computational time.

The classical linear reduced order model worked out in the frequency domain was proposed by Scanlan and Tomko [21]. This widely used section model concept has been developed into a linear aero-elastic model with the introduction of the modal aerodynamic derivatives by Szabo et al. [16]. A promising nonlinear reduced order model based on the Volterra-series technique was proposed by Wu and Kareem [22] for vortex shedding problems of bridge decks. The same approach was utilized by Balajewicz and Dowell [23] for wing flutter as well. The Volterra-series were combined with section model approach only, no aero-elastic application has been made so far. Both the Scanlan and Volterra models handle the structural motion and the fluid flow separately. In some cases, however, FSI simulations are preferred for their capabilities of simulating complex physical phenomena in the time domain. Hence, the FSI computational time reduction is a widely researched topic in the field of numerical aerodynamics. The special features of the coupled simulations are concluded below.

A crucial part of an FSI is the coupling of the solid and the fluid domains of the problem. Depending on coupling or separating the system matrices of the solid and fluid fields, monolithic and staggered methods are available. As the staggered method seems easier to implement, it gained ground instead of the monolithic (Hübner et al. [24]) concept. In case of the staggered method, both implicit and explicit approaches are used. Implicit coupling requires internal iteration within a coupling time step. Implicit scheme is referred to as strong coupling, as the imbalance of the forces and displacement is controlled at each time step. Implicit approach is particularly necessary when the CFD time step is allowed to be rather large; numerical instability or inaccuracy may occur without iteration within a time step. Zhang and Gay [25] proposed two types of implicit coupling; both a fourth order Runge-Kutta and

a predictor-corrector scheme proved to be appropriate to perform within a time step. One another method is a full sub-iteration at a time step until the predefined convergence is satisfied. It is important to emphasize that each one needs recalculation of the aerodynamic forces at each time step. The loosely coupled explicit technique is also widely used for its simplicity and the possibility to be embedded into a commercial CFD code. Despite the fact that numerical stability and accuracy is conditional, that is well concluded by Farhat et al. [20], the loosely coupled approaches can provide accurate results. It is clear that the proper time advancement scheme is of utmost importance to choose when using explicit method. Due to its simplicity, the leap-frog method is popular to solve structural dynamics, by which second order accuracy can be guaranteed [26–28]. The concept of the leap-frog method is a half-time shift between the structural unknowns (acceleration, displacement and velocity). To conclude, flutter modelling of a bridge deck or a wing of an airplane seems feasible by using full aero-elastic FSI simulations. The main drawback of these methods is the extremely high computational time that hinders their practical application.

In this paper a novel hybrid scaling technique is presented that offers full aero-elastic modelling capabilities. A scaling is applied to the CFD part of the FSI, therefore the fluid forces are calculated at lower Reynolds-number than real. In return, the computational time can be remarkably reduced that is of primary importance in industrial projects, particularly during preliminary design. The applicability of the proposed method is demonstrated on the one-degree-of freedom flutter (often mentioned as torsional instability) motion of the first Tacoma Narrows Bridge.

2 Introduction of the hybrid scaling method

The novel method consists of the ordinary modelling steps; a numerical finite element method (FEM) and a CFD model are necessary to build first. The FEM model is used to extract the dynamic mode shapes and the corresponding natural frequencies, which are further applied within the CFD code in order to perform the FSI simulation. The point in the hybrid scaling method is that the structural dynamics equations are solved with respect to the real mechanical properties, but the CFD model is considered with downscaled geometry, higher wall boundary oscillation frequency and scaled inflow wind speed compared to real. The modifications in the CFD modelling are done with respect to the reduced wind velocity (U_{red}), which is to be equal to the prototype. The special considerations are expressed below.

2.1 Fluid dynamics model

The CFD mesh needs to be constructed around the bridge deck shape. Compared to conventional unscaled approaches, the CFD environments are set by introducing three scaling parameters. These are S_{GEOM}, S_{FREQ} and S_{WIND} that belong to the geometrical dimensions, the oscillation frequencies and the inflow wind velocity; respectively. The CFD mesh geometrical size is downscaled based on the S_{GEOM} parameter; instead of the real geometry, the structure is represented with reduced size. The structural oscillation frequencies of the certain modes calculated by the FEM model are also scaled in the CFD model based on the S_{FREQ} parameter. The real inflow wind speed is scaled by using S_{WIND}. The ordinary principles as to the CFD model need to be respected. The cell point motion is to be handled with special care in order to maintain good mesh quality throughout the whole FSI process. A three-zone dynamic mesh approach is proposed in Fig. 1. The 3D mesh is to be constructed by extruding a 2D mesh, resulting in a number of 2D slices. For each of these 2D segments the following applies. The inner rigidly moving zone contains the bridge boundary and a surrounding region. Within this zone there is node motion but there is no cell distortion. The outer fix zone is perfectly standstill; no cell node motion happens at all. The transition deforming zone accommodates the deformation difference between the inner and outer zones. A simple linear (user defined) function is applied to diminish the cell motion from the outer edge of the rigidly moving zone towards the inner edge of the fixed zone.

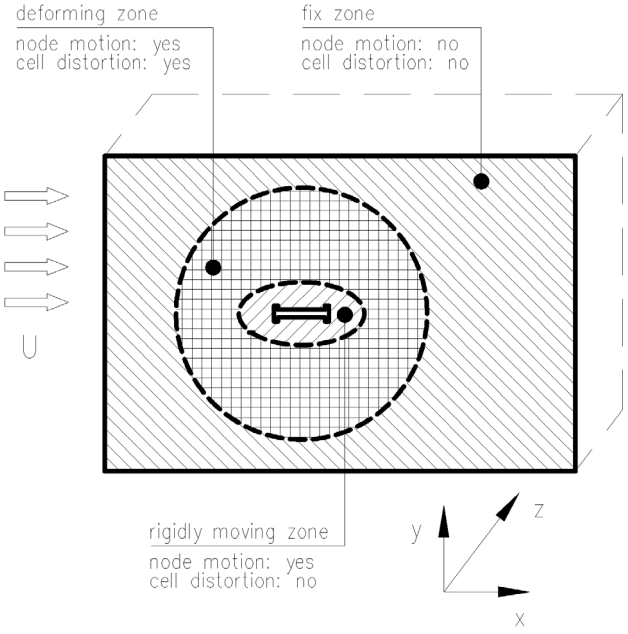

Fig. 1 Three zone types for the aero-elastic CFD mesh

Obviously, the 3D cells between two neighboring 2D segments have to deform. If the boundary motion is extremely large, more complex dynamic mesh can be recommended based on minimizing a functional such as proposed by Ge and Liu [29] or assuming the fluid domain as a pseudo-solid structure by Zhong and Xu [30].

2.2 Mechanical model and steps of the simulation

The FSI simulation was carried out by using a staggered, explicit scheme (see Fig. 2), which is described in [20]. The proposed method requires the scaling parameters (S_{GEOM}, S_{WIND} and S_{FREQ}). In Fig. 2, *u*: structural displacement, *f*: modal force, *x*: bridge CFD boundary displacement, *w*: fluid unknowns. The modelling steps are addressed below:

1. Calculation of the modal forces:

The modal aerodynamic forces acting on the CFD bridge deck boundary of a section are calculated at every coupling time step (Fig. 3). Based on our preliminary study, the friction forces were neglected for simplicity. It is important to underline that by involving modal analysis in the FSI, the time costly mapping of the aerodynamic forces onto the structure surface mesh can be omitted. The structural motion is computed based on the modal analysis; the problem can be reduced by using the mode shapes and natural frequencies of the bridge. The dynamic equation of motion can be converted to scalar equations by using the well-known modal transformations. The number of the modal equations depends on that of the included mode shapes. In case of a bending and a torsion modes considered, the modal forces based on the aerodynamic pressure forces from the CFD can be written in Eqs. (1) and (2) according to Fig. 3. The Φ_{disp} and Φ_{rot} are the mode shape vectors of the bridge deck. *L* is the total length of the deck.

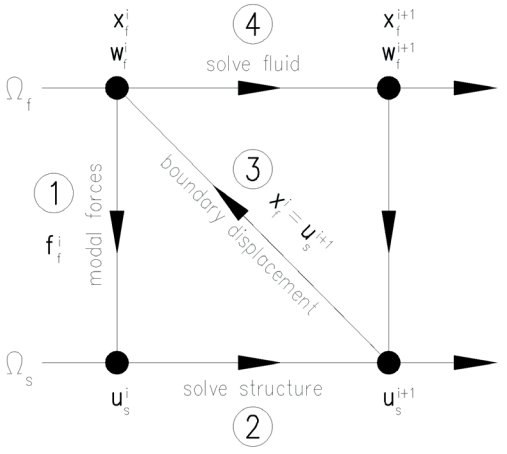

Fig. 2 Staggered, explicit fluid-structure coupling chart

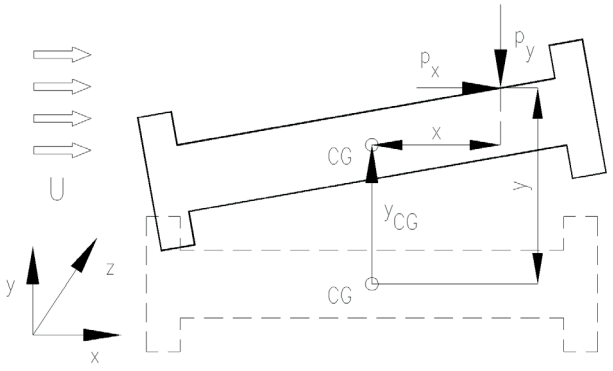

Fig. 3 Aerodynamic pressure representation on a slice of the 3D deck

$$f_{disp} = \iint \Phi_{disp}(z) \times p_y(x,z)\,dxdz \tag{1}$$

$$f_{rot} = \iint \Phi_{rot}(z) \cdot x \cdot p_y(x,z)\,dxdz + \iint \Phi_{rot}(z) \cdot p_x(x,z) \cdot (y - y_{CG})\,dydz \tag{2}$$

The modal forces are scaled up to the real bridge as:

$$f_{disp,REAL} = (S_{GEOM})^2 \cdot (S_{WIND})^2 \cdot f_{disp,CFD}, \tag{3}$$

$$f_{rot,REAL} = (S_{GEOM})^3 \cdot (S_{WIND})^2 \cdot f_{rot,CFD}. \tag{4}$$

2. Solving the structural equations:

The structural displacement (*u*) of the real structure is determined based on the modal analysis combined with the leapfrog method with a time step of:

$$\Delta t_{REAL} = S_{FREQ} \cdot \Delta t_{CFD}. \tag{5}$$

3. Transferring bridge displacement to the CFD:

The calculated real bridge bending (*h*) and torsion displacement (α) scaled down into the CFD boundary:

$$x_h^i = \frac{1}{S_{GEOM}} u_h^{i+1}, \tag{6}$$

$$x_\alpha^i = u_\alpha^{i+1}. \tag{7}$$

4. Solving fluid equations:

Constructing the CFD mesh, setting the boundary conditions and the numerical schemes and choosing a proper turbulence model. The geometrical size (*B* and *D*: bridge deck width and height, *L*: span length), the inlet wind speed (*U*) and the oscillation frequencies (*n*) in the CFD simulation are scaled down based on the above selected scaling parameters:

$$B_{CFD} = \frac{1}{S_{GEOM}} B_{REAL}, \tag{8}$$

$$D_{CFD} = \frac{1}{S_{GEOM}} D_{REAL}, \tag{9}$$

$$L_{CFD} = \frac{1}{S_{GEOM}} L_{REAL}, \tag{10}$$

$$U_{CFD} = \frac{1}{S_{WIND}} U_{REAL}, \tag{11}$$

$$n_{CFD} = S_{FREQ} \cdot n_{REAL}. \tag{12}$$

As there is no iteration between the fluid and solid domains, the step number 2 needs to be performed by selecting the most appropriate time integrator for calculating the structural unknowns. The second order time accurate leap-frog scheme was utilized [26]. By using modal analysis, independent scalar equations are to be solved that can be embedded into the fluid solver. Hence, the fluid-structure interaction calculation requires insignificant CPU time within a time step.

3 Numerical example

3.1 The first Tacoma Narrows Bridge

The proposed procedure is demonstrated on a well-known case; the torsional oscillation of the 1st Tacoma Narrows Bridge. The geometry and the mechanical properties of the bridge structure were taken from [31]. The structure was a suspension bridge with main cables and hangers. The pylons were made of pure steel. The bridge deck consisted of two I-shape girders on each side, which were connected together by cross girders. A concrete slab was placed onto the cross girders as a carriageway. The simulation was carried out with the guidance of video documentations. According to observations, the bridge showed dominantly torsional oscillation, with a corresponding period of approximately $T = 5$ s, which indicates an oscillation frequency of around $n = 0.20$ Hz. Based on the studies found in literature, the following conclusions can be drawn as to the observed phenomenon:

- The oscillation was caused neither by gust nor vortex shedding related resonance
- The primary reason of the bridge deck oscillation can be explained by the mutual interaction of the structural motion and the aerodynamic forces, finally resulted in a negative total damping over the critical wind speed
- The critical wind speed was low due to the unfavorable bridge deck section shape and the low torsional stiffness
- The first torsion mode showed up alone before the bridge collapsed, therefore the phenomenon is referred to as single DOF torsional instability instead of coupled flutter, which occurs in case of streamlined objects

3.2 Structural dynamics model of the bridge

The FEM model of the bridge was built up by using the AXIS [32] commercial software (Fig. 4) based on the bridge drawings [31]. The main cables and the hangers were modelled by using truss elements with compression-tension capabilities. Beam elements were applied for the stiffening girders and the cross girders. The concrete slab was modelled by using shell elements. The stiffness of the structural elements were calculated based on the Young-modulus of steel ($E = 20600$ kN/cm^2), and concrete (C20/25 grade assumed, $E = 2000$ kN/cm^2).

The dynamic mode shapes and the corresponding natural frequencies (Figs. 5 and 6) were calculated by taking the second order effect of the tension in the main cables into account, that is the initial stresses in the cables are included in the stiffness matrix. This linear approach was selected as the aim was to find the flutter onset. If the amplitudes over the critical wind speed are of interest, however, nonlinear structural models are used [33].

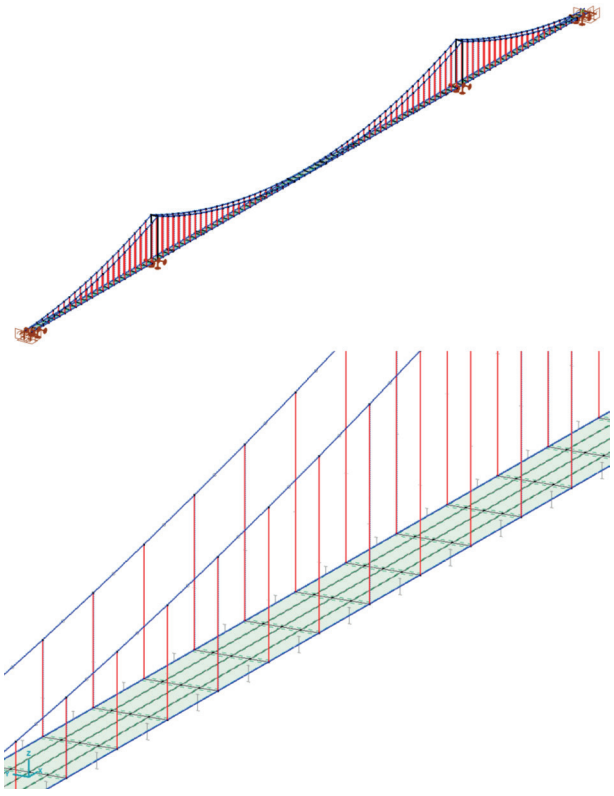

Fig. 4 Structural FEM model

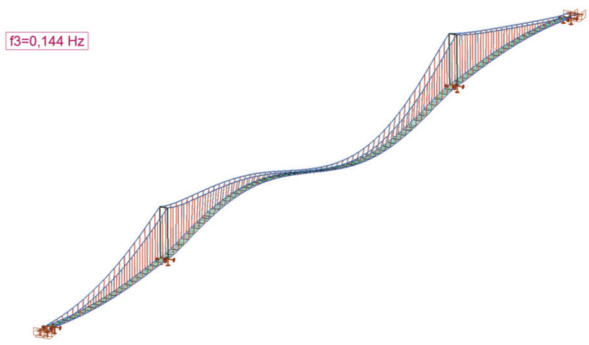

Fig. 5 Vertical bending mode

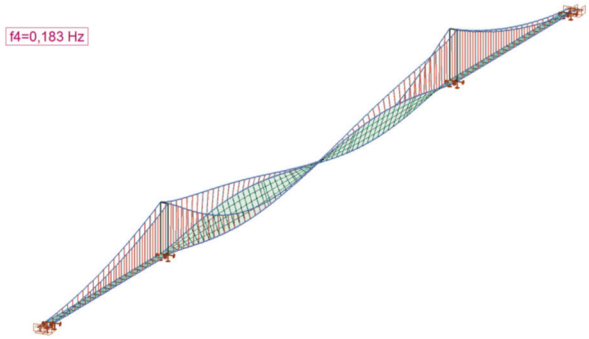

Fig. 6 Torsion mode

The results are in good agreement with that can be found in literature (Billah and Scanlan [3]); the natural frequency belonging to the most relevant torsional mode is $n = 0.183$ Hz.

It is an important issue to assume the structural damping properly. The real value of the Tacoma Narrows bridge is not known [3], therefore the logarithmic decrement of structural damping is assumed to be $\delta = 0.02$ for each mode (Figs. 5–6).

3.3 CFD model of the bridge

The proposed technique can be applied either to 2D or 3D CFD meshes. The latter is applied here (Fig. 7). The mesh was made by constructing a 2D mesh around the bridge deck shape with triangular cells. The number of the in-plane cells is ~25.000. The three-dimensional mesh was made by extruding the 2D mesh with a division number of 100, resulting in a total number of 2.5 million cells. The LES turbulence model was utilized. First order advancement scheme was selected for time discretization. A coarse mesh by using ~10.000 in-plane cells and 10 extrusion division number resulting in a total cell number of 100.000 was also created. This mesh was combined with the k-ε turbulence model. Even if the two applied turbulence models are different in nature, their results were compared; the k-ε model was validated to the LES. The aim of the coarse mesh is the low CPU time in order to demonstrate the hybrid scaling more detailed with several simulations. It was shown that RANS models can be good compromise between accuracy and low CPU time for flutter problems [34–35]. The computational domain is shown in Fig. 8.

The geometric scaling parameter S_{GEOM} was selected to 10, which means that the width of the deck is $B = 1.243$ m in the CFD model, while $B = 12.43$ m in case of the real bridge. The diameter of the inner and outer circles around the bridge (see Fig. 1) are $D_1 = 7$ m and $D_2 = 15$ m, respectively.

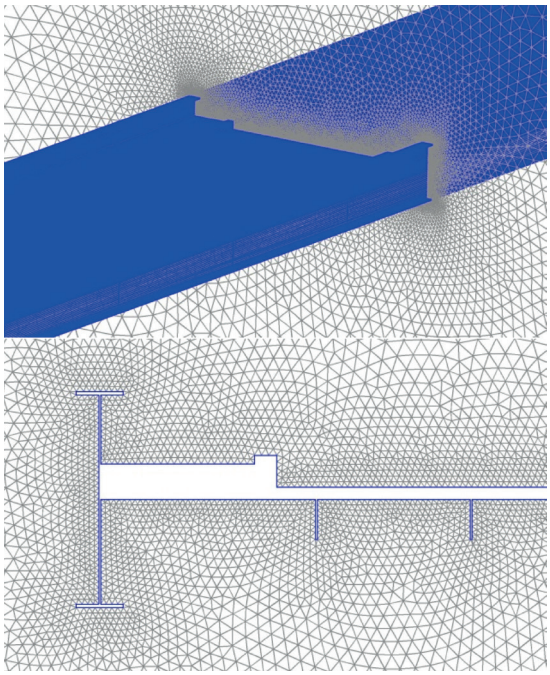

Fig. 7 2D slice of the 3D CFD mesh around the bridge deck

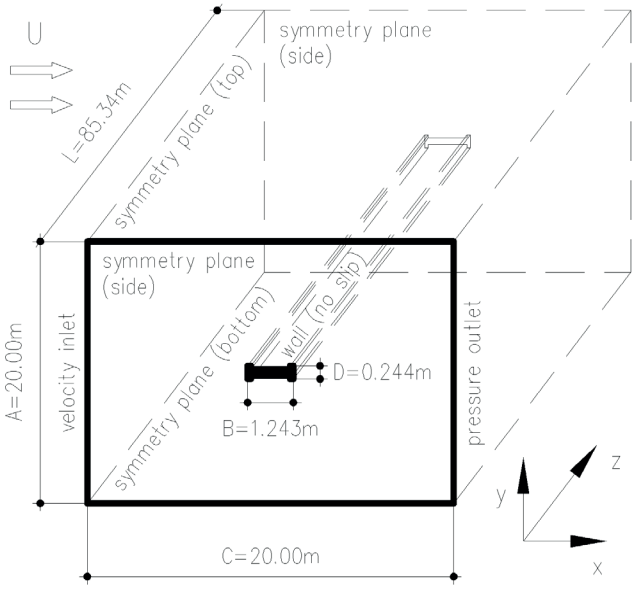

Fig. 8 Scaled ($M = 1{:}10$) CFD domain of the main span of the bridge deck

The displacement and the displacement-dependent aerodynamic forces are irrelevant at the side spans, therefore the CFD model includes the main span only. Steady, uniform wind speed and turbulent properties were defined at the inlet boundary. The turbulence intensity and length scale were 1 % and 0.1 m.

3.4 Hybrid scaling

The hybrid scaling parameters for the FSI simulation can be seen in Table 1. For better understanding, a setup without scaling is also presented separately in Table 2. In the tables below B: bridge deck width, D: bridge height, L: main span length, U: inflow wind speed, n: natural frequency of the torsional mode, $U_{red} = U/(Bn)$: reduced wind velocity, Re: Reynolds-number, Δt: time step, N: total time step number in the FSI simulation, T: end time. The scaling parameters were intuitively selected as follows (Table 1): $S_{GEOM} = 10$, $S_{WIND} = 1$ and $S_{FREQ} = 10$.

Once the frequency and wind speed scaling parameters are chosen, the geometry scaling parameter is not arbitrary in order to maintain the reduced wind velocity value belonging to the real case. Based on the above selected scaling parameters, the geometry of the real bridge was downscaled in the CFD mesh, while the inflow wind velocity was not changed. The oscillation frequency of each mode shape of the bridge is 10 times higher in the CFD than the real case; the natural frequency of the torsion mode of the bridge is $n = 0.18$ Hz, which is equivalent to $n = 1.80$ Hz in the CFD. The time step size was set to $\Delta t = 0.001$ s in the CFD that satisfies the CFL criteria in the majority of the domain. As a consequence of the hybrid scaling, the time step of the structural dynamics is not equal to that of the CFD; applying the frequency scaling parameter $S_{FREQ} = 10$, the time step size in the structural dynamics solution was $\Delta t = 0.01$ s, 10 times higher than the CFD time step. Consequently, the end time in the CFD and the structural dynamics is also different; $T = 10$ s and $T = 100$ s; respectively.

By studying to the scaled and unscaled cases (Tables 1 and 2), the benefits of the hybrid scaling are clear. If no scaling is applied, the time step needs to be set to $\Delta t = 0.001$ s both for the CFD and the structural dynamics scheme, leading to a total number of time steps of $N = 10^5$, 10 times higher than that of the scaled case (Table 1). On top of all, without scaling, the Reynolds number is higher in the CFD model, leading to higher y+ values at the wall region. This may require denser boundary layer mesh. Naturally, the scaling brings the Reynolds-number scaling problem into the hybrid method, which always needs to be assessed.

Table 1 Scaling parameters of the FSI with scaling

		REAL	FSI FLUID	FSI SOLID
S_{GEOM}	[-]		10	
B	[m]	12.43	1.243	-
D	[m]	2.44	0.244	-
L	[m]	853.4	85.34	-
S_{WIND}	[-]		1	
U	[m/s]	15	15	-
S_{FREQ}	[-]		10	
$n_{TORSION}$	[Hz]	0.18	1.80	0.18
U_{RED}	[-]	6.70	6.70	-
Re	[-]	5.5E + 08	5.5E + 07	-
Δt	[s]	-	0.001	0.01
$N = T/\Delta t$	[-]	-	**1.0E + 04**	**1.0E + 04**
T	[s]	100	10	100

Table 2 Scaling parameters of the FSI without scaling

		REAL	FSI FLUID	FSI SOLID
S_{GEOM}	[-]		1	
B	[m]	12.43	12.43	-
D	[m]	2.44	2.44	-
L	[m]	853.4	853.4	-
S_{WIND}	[-]		1	
U	[m/s]	15	15	-
S_{FREQ}	[-]		1	
$n_{TORSION}$	[Hz]	0.18	0.18	0.18
U_{RED}	[-]	6.70	6.70	-
Re	[-]	5.5E + 08	5.5E + 08	-
Δt	[s]	-	0.001	0.001
$N = T/\Delta t$	[-]	-	**1.0E + 05**	**1.0E + 05**
T	[s]	100	100	100

4 Results

The FSI simulation requires initial conditions both for the CFD and the structural dynamics domains. In the CFD the initial values (inflow wind speed, turbulence properties) were kept constant. In the structural dynamics, a perturbation was applied; each mode was excited within the first 100 time step, then the added modal forces were switched off. The reached initial vertical displacement was 1.05 m, the rotation 10.3 deg, which are large enough to generate self-excited forces and observe the decay motion. Though a free development of the unstable motion would be desirable, the perturbation accelerates the simulation, and torsional instability motion can accurately be captured. The most relevant result of the FSI simulation is the time-series of the bridge deck displacement.

In the case of the Tacoma Narrows Bridge the torsion motion of the bridge deck is important to study. In Fig. 9 the torsion amplitude of the quarter section of the main span can be seen, by using LES combined with the fine mesh (2.5 *M* cells). The decay motion was investigated at different inlet wind velocities of 5, 10 and 15 m/s. The total damping of the vibrating deck in airflow becomes zero at around 9 m/s, which is close to the critical wind speed of the torsional instability. The deformed deck from the 3D FSI simulation can be seen in Fig. 10. Although three modes (sway, bending and torsion) were included in the modal structural dynamics calculation, only the torsion mode dominates in the unstable oscillation, which is well in line with the experiences (Fig. 11). It should be noted that the torsion displacement time series computed on the coarse mesh combined with k-e model were close to that of the fine mesh with LES.

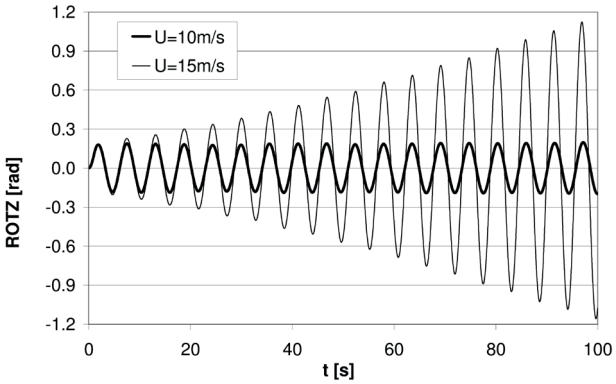

Fig. 9 Time history of the maximum rotation of the deck

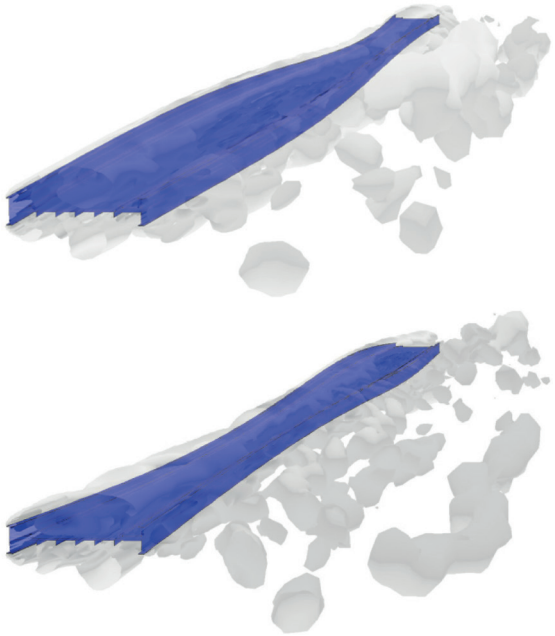

Fig. 10 Deformed stages of the main span in the CFD simulation

As demonstrated in Fig. 10, the proposed novel hybrid technique is appropriate to model aero-elastic problems. The main advantage of the method is that the structural motion can be investigated in detail, leading to better understanding of the phenomenon. In Fig. 12 the bridge deck deformation can be seen [36]. It can be observed that besides torsion, sway and vertical bending motion components are also present, but their role is marginal, though. The sway motion is explained by the drag force change due to the torsion motion and the consequently varying wind loaded height. This kind of horizontal motion can be well observed in the videos of the bridge oscillation. The bending motion also develops due to the aerodynamic coupling of the torsion and bending modes, even if this coupling is weak.

In the aftermath of the tragedy of the Tacoma Narrows Bridge, basically two different countermeasures have been developed and applied in the bridge deck shape design.

Fig. 11 Deformed positions of the real bridge deck

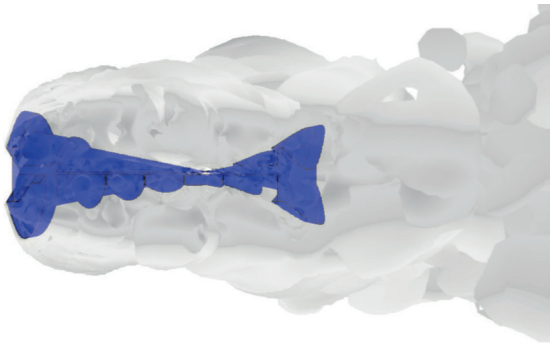

Fig. 12 Spatially deformed bridge deck with vortices around it

The stiffening girder is made of either a truss structure [37–38] or a streamlined box girder [39–40]. In case of the Tacoma Narrows Bridge, additional aerodynamic elements could have improved the stability, which is practically interesting for bridge design engineers. Therefore, in order to demonstrate the capabilities of the proposed hybrid method, two other bridge deck sections were also simulated besides the original Tacoma case. The three studied shapes are shown in Fig. 13. The TAC is the original shape, the TAC-STREAM is the bridge deck with aerodynamic modification on the upwind and downwind sides of the deck, and the STREAM is a fully closed box girder. The coarse mesh strategy along with the k-ε turbulence model (around 100.000 cells) was applied to these lots of cases. From practical point of view, the TAC-STREAM version could have been constructed, but the STREAM case would have altered the level of the carriageway.

Though practical feasibility of the STREAM version is not investigated, still considered for gaining experiences. All the three cases were combined with the original structural dynamic properties assuming that the modifications have little contribution to the mechanical properties. The aerodynamic instability of the Tacoma Bridge with these three cross sections was studied in detail. Besides the hybrid FSI, the aerodynamic derivatives introduced by Scanlan and Tomko [21] were computed. The $A2^*$ derivatives [5, 8, 14, 38] of the investigated cross sections can be seen in Fig. 14 extended with that of the Theodorsen's theory. It can be seen that the $A2^*$ (the connection between the torsional motion and the moment) turns to be positive (leading to negative torsional damping) in case of the TAC shape and even by using wind noses, the TAC-STREAM shape performs badly. The proper stabilization can be achieved by using STREAM shape.

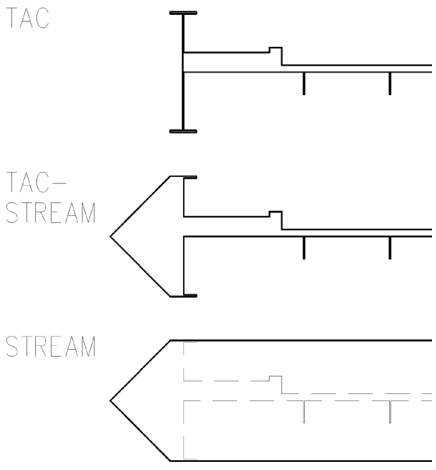

Fig. 13 Aerodynamic modifications

The total damping of the bridge structure in airflow with the three different bridge deck shapes is illustrated in Fig. 15. The total logarithmic decrement of damping was determined based on the modal aerodynamic derivatives method proposed by Szabo et al. [16]. The bridge deck is given a forced three-dimensional oscillation according to the relevant mode shapes, therefore can be regarded as an equivalent counterpart of the FSI, only in the frequency domain. The total damping curves of the eigenvalue analysis are in good agreement with those of the FSI simulation. The critical wind velocities based on the FSI were extracted by linear interpolation as: U_{cr} = 9.0, 12.4 and 20.0 m/s for the TAC, TAC-STREAM and STREAM sections; respectively. The bridge deck torsion motion was calculated by using modal analysis with 3 modes (3DOF) and only one mode (1DOF) included.

In Figs. 16–18, important consequences can be drawn. In case of the TAC the torsion mode dominates. The torsional amplitudes are identical by using all the three modes and one torsion mode only. This finding proves that the Tacoma Narrows Bridge oscillation was torsional instability, and no contribution of the bending mode was important. The TAC-STREAM case was slightly different: at the

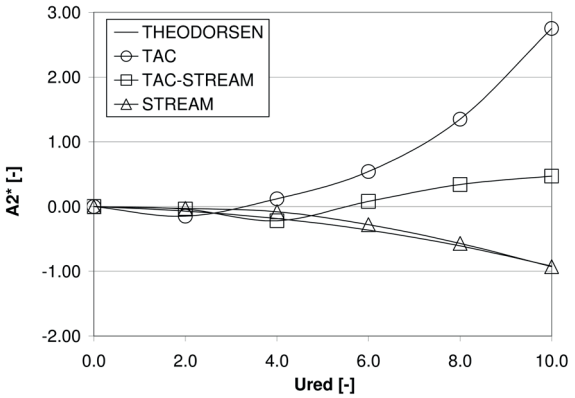

Fig. 14 Aerodynamic derivative $A2^*$

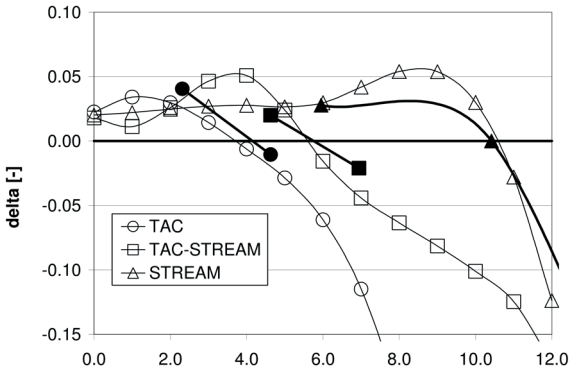

Fig. 15 Total damping of the torsional modes of the three bridge deck shapes (thin lines: eigenvalue, thick lines: FSI)

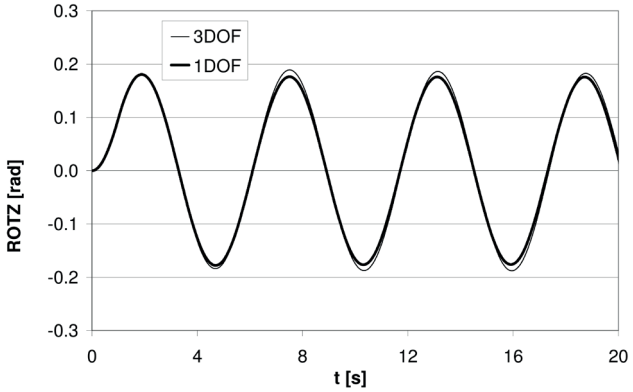

Fig. 16 Torsion amplitudes at U = 10 m/s (bridge deck: TAC)

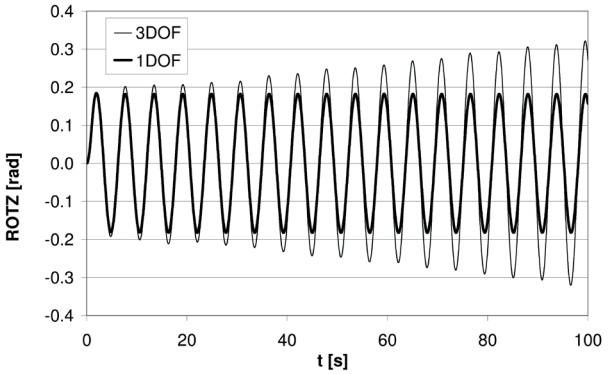

Fig. 17 Torsion amplitudes at U = 15 m/s (bridge deck: TAC-STREAM)

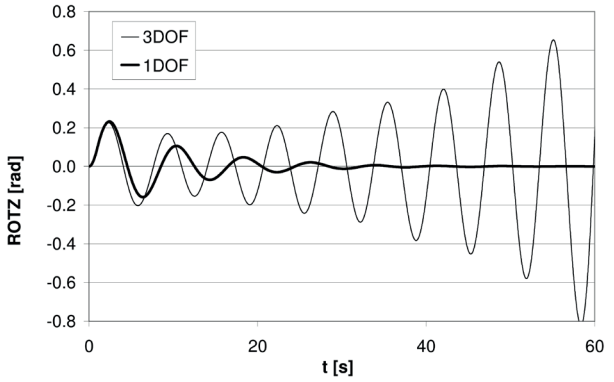

Fig. 18 Torsion amplitudes at U = 30 m/s (bridge deck: STREAM)

wind speed of U = 15 m/s, there is a noticeable difference between the torsion amplitude time series by using three modes and only one. This means that there is a little coupling effect between the modes through the aerodynamic forces. In case of the STREAM case the mode coupling effect was significant; at U = 30 m/s the motion amplitudes grow rapidly with all the three modes but decreases fast with the torsion mode only. The mode coupling for the STREAM section is dominant; as the $A2^*$ is negative for all U_{red} values, no instability can occur without the vertical bending mode included.

The torsional and bending amplitude time series of the quarter section of the bridge can be seen in Figs. 19–21. In case of the TAC section the torsion amplitudes are growing exponentially (Fig. 19) at the wind speed of U = 15 m/s, over the critical value (U_{cr} = 9.0 m/s). The bending motion amplitude, however, do not follow this tendency, which is in line with the finding that the bending mode is not relevant. The TAC-STREAM case is different. The growth in the torsion amplitude at the wind speed of U = 20 m/s is followed by the bending amplitude until t = 70 s, but after this time instance the bending motion tends to decay. This means that there is indeed some coupling between the torsion and bending modes, but this effect is marginal, nevertheless. The STREAM case is an ideal example to coupled flutter. Over the critical wind speed the exponentially growing torsion amplitude is perfectly accompanied by similarly growing bending amplitudes.

The critical wind velocities based on the FSI are: U_{cr} = 9.0, 12.4 and 20.0 m/s for the TAC, TAC-STREAM and STREAM sections; respectively. The torsion instability of the TAC (original bridge) is dangerously low. It can be seen that the TAC-STREAM modification gives only slight improvement. The problem is that the bridge deck shape cannot be remarkably stabilized, which can be observed in

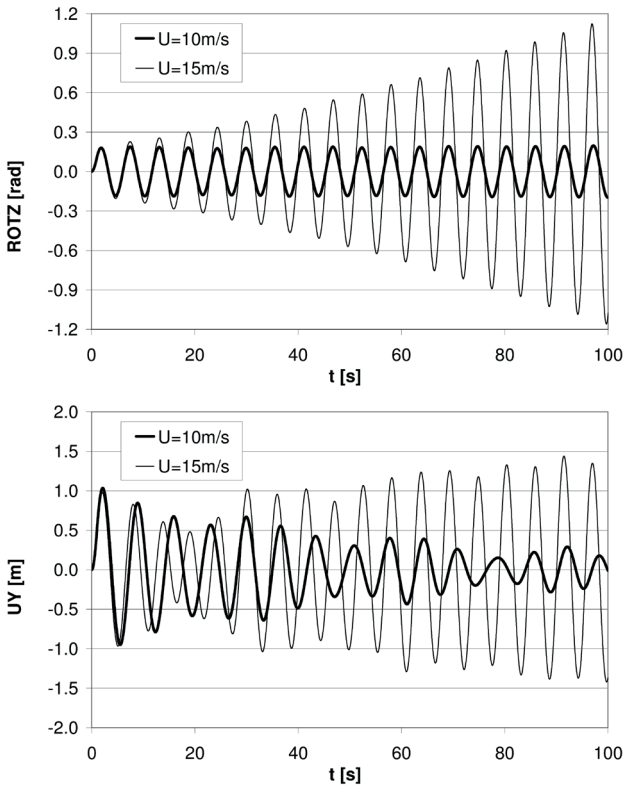

Fig. 19 Torsion and bending amplitudes of the quarter section of the main span (TAC)

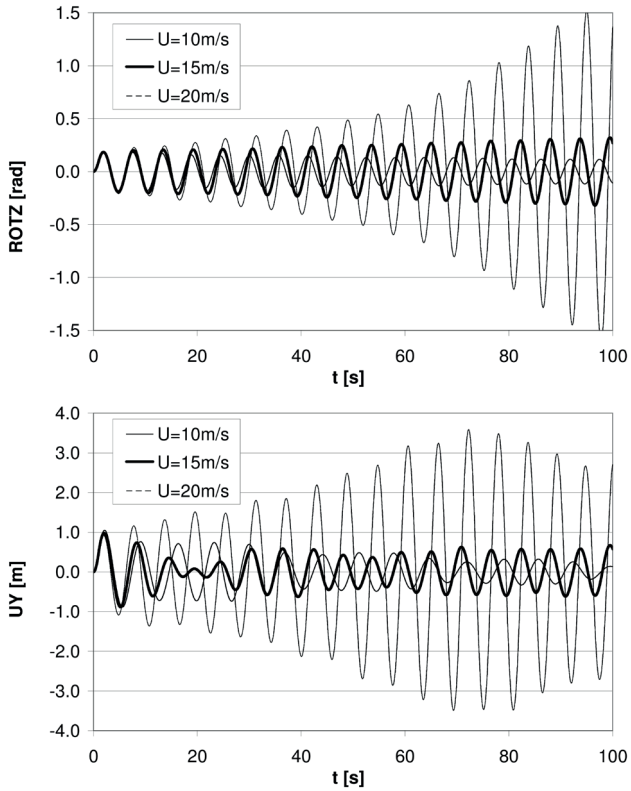

Fig. 20 Torsion and bending amplitudes of the quarter section of the main span (TAC-STREAM)

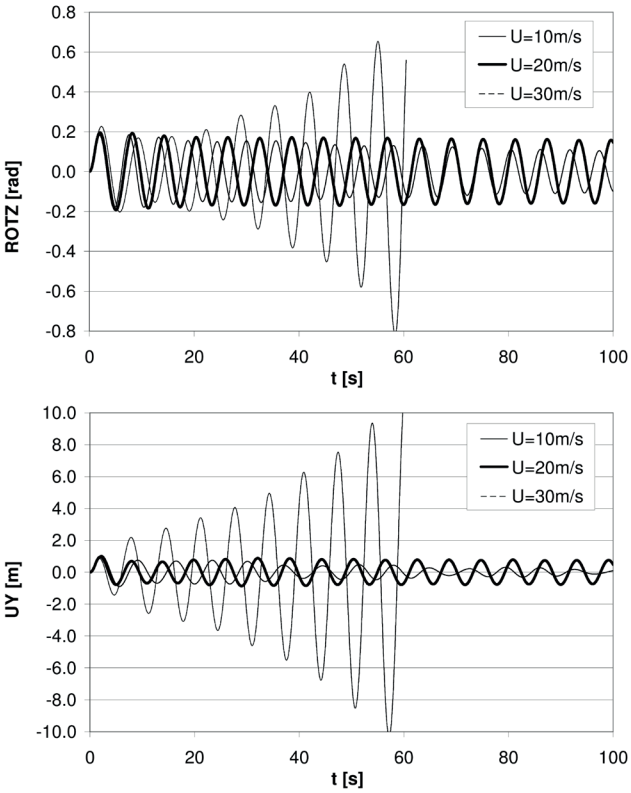

Fig. 21 Torsion and bending amplitudes of the quarter section of the main span (STREAM)

Fig. 14. The type of instability remains purely torsional. If the bridge deck is altered into the STREAM version, the critical value can be raised up to 20 m/s, which would still have not been satisfactory. The reason for that can be found when studying the mechanical properties. The ratio of the torsion (n_t = 0.183 Hz) and bending (n_h = 0.144Hz) frequencies is around $\alpha = n_t/n_h = 1.27$, which is highly unfavorable in terms of coupled flutter. In case of a streamlined flat plate (e.g. an airfoil or a streamlined bridge deck) with one torsion mode and one bending mode, the ratio of 1.27 is close to the one that gives the lowest critical flutter speed. Hence, the ratio of the torsion and bending modes of the Tacoma Narrows Bridge can be indeed regarded as fatal, but not for the original bridge configuration, as was suspected early on. In contrast, it has major relevance for the aerodynamically stable STREAM case only, which was found to be prone to mode coupled flutter instability (Fig. 22).

Having studied the possible solutions to improve the aerodynamic stability of the Tacoma Bridge deck, it should be noted that there are structures that requires inverse philosophy. Energy harvesters produce electricity on the principle of flutter motion [41]. These machineries consist of flaps that need to show flutter instability, therefore the aim is to construct structures that are prone to flutter in contrast to bridges and buildings.

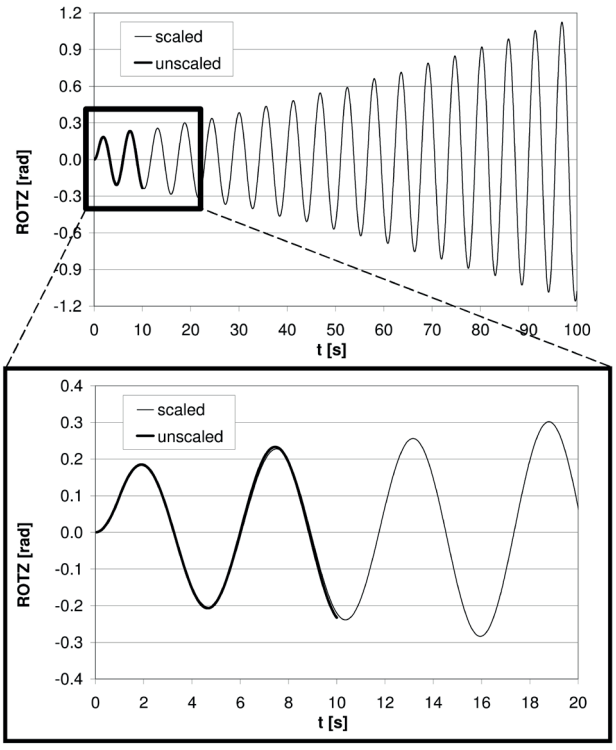

Fig. 22 Torsion and bending amplitudes of the quarter section of the main span (STREAM) with and without scaling

Finally, some details as to the computational time are given. A scaled simulation case with the coarse mesh combined with the k-ε model (N = 10.000 time steps) requires approximately 20 hours (2.4 GHz CPU, single core). The torsional amplitude time series of the real bridge structure can be seen in Fig. 22 (thin line). If no scaling is applied, the same CPU time enables ten times less length of oscillation to model. In order words, the same length would have required 200 hours CPU time, therefore has not been carried out until the end time. We note that the turbulence intensity and length scale in case of the unscaled simulation was 1 % and 1 m, respectively. The amplitudes calculated with and without scaling are in good agreement, which can be explained with the minor Reynolds-number effect. If the computed aerodynamic forces are not burdened by Reynolds-number effects, the hybrid scaling method offers equivalent results with the unscaled simulation, but at a remarkably reduced computational cost. In Fig. 23 a detail of the torsion time series can be seen belonging to the bridge boundary of the scaled CFD model and the real bridge structure at the time instance of around 8 s.

As was explained earlier, the oscillation frequencies are higher in the CFD than in the structural dynamics calculation. The time step size is adjusted accordingly in order to have the same time step number in these two domains. If the structural motion of the real bridge is extremely slow, large time step size can be allowed. As an unscaled CFD simulation requires usually small time steps, this seems only feasible by scaling the CFD model. The hybrid scaling enables to use the most adequate time step size both for the CFD and the structural dynamic calculation, resulting in less time step number necessary. That is the point in using hybrid scaling. In Fig. 24 the unscaled case can be seen. The oscillation frequencies as well as the time stepping are the same for the CFD and the structural dynamics solution. As the CFD is not scaled in this case, significantly more time steps are necessary compared to the scaled case.

5 Conclusions

In this paper a novel hybrid scaling approach was introduced that was found to be appropriate for wind engineering problems. The main goal was to work out a full

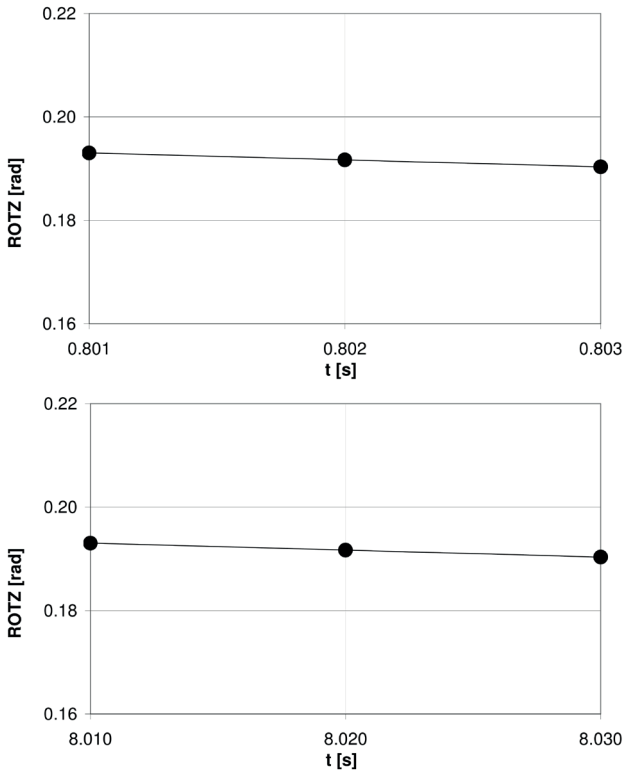

Fig. 23 Torsion amplitudes of the CFD (top) and the real bridge (bottom) with hybrid scaling
Time step sizes: Δt (CFD-SCALED) = 0.001s, Δt (REAL) = 0.01s
Periods of torsional oscillations: T (CFD-scaled) ≈ 0.5s, T (REAL) ≈ 5.0s
Time step number for a cycle: N (CFD-scaled) ≈ 500, N (REAL) ≈ 500

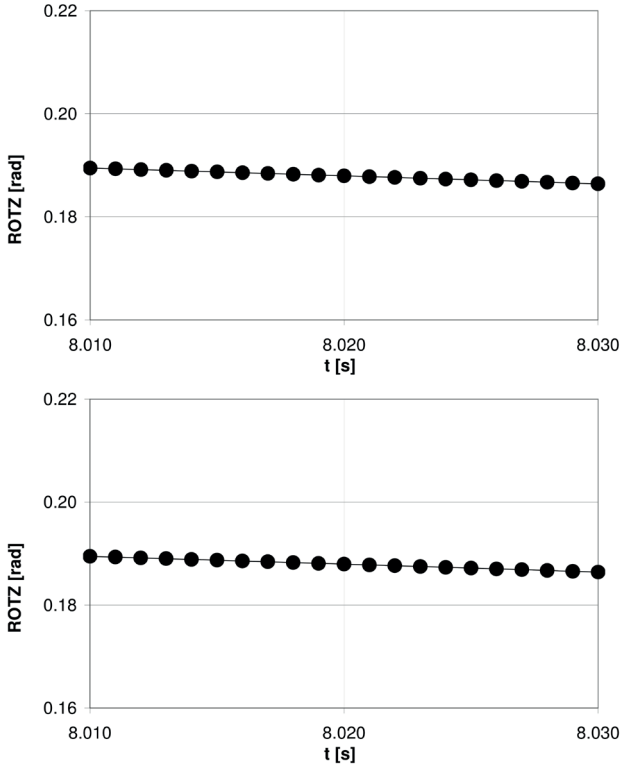

Fig. 24 Torsion amplitudes of the CFD (top) and the real bridge (bottom) without hybrid scaling
Time step sizes: Δt (CFD-SCALED) = 0.001s, Δt (REAL) = 0.001s
Periods of torsional oscillations: T (CFD-unscaled) ≈ 5.0s, T (REAL)≈5.0s
Time step number for a cycle: N (CFD-unscaled) ≈ 5000, N (REAL) ≈ 5000

aero-elastic approach for bridge deck instability assessment, which can be performed even on a low-profile PC. In the proposed procedure the whole bridge span can be considered, therefore mode coupling effect can be studied in detail. The FSI simulations were applied to the original Tacoma Narrows Bridge. The calculated critical wind speed belonging to the torsional instability and the nature of the oscillation were in good agreement with experiences. The proposed FSI was tested on modified bridge deck shapes as well, in order to design aerodynamically stabilized sections.

It was shown that the hybrid scaling can provide results equivalent with unscaled FSI approaches, but at a remarkably reduced computational cost. Based on the findings of this paper, the hybrid FSI method can be proposed to aerodynamic instability related problems in aerospace or bridge engineering. The method was demonstrated for torsional instability and coupled flutter, in which the inflow wind speed was idealized as constant. If buffeting is to be modelled, however, time and space varying wind speed needs to be used at the inlet in the CFD model. Likewise, bridge deck instabilities modelling may also require unsteady flow conditions to consider. In these cases, besides the mean wind speed, the turbulent inlet properties are to be scaled as well, which needs further development of the hybrid scaling method.

Acknowledgements

The authors are grateful for the support of the Department of Fluid Mechanics (University of Technology and Economics, Budapest), CFD.hu Ltd., Pont-TERV Ltd. and the INNOCSEKK PLUS foundation (NKTH, Hungary).

References

[1] Farquharson, F. B. (ed.) "Aerodynamic Stability of Suspension Bridges", University of Washington Engineering Experiment Station, 116, 1949.

[2] Goller, R. R. "The Legacy of 'Galloping Gertie' 25 Years After", Civil Engineering, pp. 50–53, 1965.

[3] Billah, K. Y., Scanlan, R. H. "Resonance, Tacoma Narrows bridge failure, and undergraduate physics textbooks", American Journal of Physics, 59(2), pp. 118–124, 1991. https://doi.org/10.1119/1.16590

[4] Miyata, T., Yamaguchi, K. "Aerodynamics of wind effects on the Akashi Kaikyo Bridge", Journal of Wind Engineering and Industrial Aerodynamics, 48(2–3), pp. 287–315, 1993. https://doi.org/10.1016/0167-6105(93)90142-B

[5] Miyata, T., Yamada, H., Boonyapinyo, V., Santos, J. C. "Full model testing of large cable-supported bridges", In: Proceedings of the 9th International Conference on Wind Engineering (ICWE1995), New Delhi, India, 1995, pp. 249–280.

[6] Larsen, A. "Aerodynamics of the Tacoma Narrows Bridge - 60 years later", Structural Engineering International, 10(4), pp. 243–248, 2000. https://doi.org/10.2749/101686600780481356

[7] Ge, Y., Xia, J., Zhao, L., Zhao, S. "Full Aeroelastic Model Testing for Examining Wind-Induced Vibration of a 5000m Spanned Suspension Bridge", Frontiers in Built Environment, 4(20), 2018. https://doi.org/10.3389/fbuil.2018.00020

[8] Starossek, U., Aslan, H., Thiesemann, L. "Experimental and numerical identification of flutter derivatives for nine bridge deck sections", Wind and Structures, 12(6), pp. 519–540, 2009. https://doi.org/10.12989/was.2009.12.6.519

[9] Haque, Md. N., Katsuchi, H., Yamada, H., Nishio, M. "Flow field analysis of a pentagonal-shaped bridge deck by unsteady RANS", Engineering Applications of Computational Fluid Mechanics, 10(1), pp. 1–16, 2016. https://doi.org/10.1080/19942060.2015.1099569

[10] Šarkić, A., Fisch, R., Höffer, R., Bletzinger, K.-U. "Bridge flutter derivatives based on computed, validated pressure fields", Journal of Wind Engineering and Industrial Aerodynamics, 104–106, pp. 141–151, 2012. https://doi.org/10.1016/j.jweia.2012.02.033

[11] Attia, W. A. L., Aziz Ahmed, A. A. "Aero-elastic Investigation of Long Span Suspension Bridge Decks by Numerical CFD and FSI Analyses", Civil and Environmental Research, 8(7), pp. 81–90, 2016. [online] Available at: https://www.iiste.org/Journals/index.php/CER/article/view/31594

[12] Abbas, T., Kavrakov, I., Morgenthal, G. "Methods for flutter stability analysis of long span bridges: a review", Proceedings of the Institution of Civil Engineers - Bridge Engineering, 170(4), pp. 271–310, 2017. https://doi.org/10.1680/jbren.15.00039

[13] Woojin, K., Haecheon, C. "V0076: Process of the collapse of the Tacoma Narrows Bridge", presented at 70th Annual Meeting of the APS Division of Fluid Dynamics, Denver, CO, USA, Nov, 19–21, 2017. https://doi.org/10.1103/APS.DFD.2017.GFM.V0076

[14] Ge, Y. J., Xiang, H. F. "Computational models and methods for aerodynamic flutter of long-span bridges", Journal of Wind Engineering and Industrial Aerodynamics, 96(10–11), pp. 1912–1924, 2008. [online] https://doi.org/10.1016/j.jweia.2008.02.017

[15] Chen, S. R., Cai, C. S., Chang, C. C., Gu, M. "Modal coupling assessment and approximated prediction of coupled multimode wind vibration of long-span bridges", Journal of Wind Engineering and Industrial Aerodynamics, 92(5), pp. 393–412, 2004. https://doi.org/10.1016/j.jweia.2004.01.004

[16] Szabo, G., Gyorgyi, J., Kristof, G. "Advanced flutter simulation of flexible bridge decks", Coupled Systems Mechanics, 1(2), pp. 133–154, 2012. https://doi.org/10.12989/csm.2012.1.2.133

[17] ANSYS "Ansys Fluent" [computer program] Available at: https://www.ansys.com/products/fluids/ansys-fluent

[18] Szabó, G., Kristóf, G., Pálossy, M. "On a novel three-dimensional fluid-structure interaction technique application to a pedestrian bridge with a main span of 120m", In: 6th International Symposium on Wind Engineering, Hamburg, Germany, 2014, pp. 372–373. [pdf] Available at: https://www.ruhr-uni-bochum.de/cwe2014/dwnld/CWE2014_AbstractBook.pdf

[19] Courant, R., Friedrichs, K., Lewy, H. "On the Partial Difference Equations of Mathematical Physics", IBM Journal of Research and Development, 11(2), pp. 215–234, 1967. https://doi.org/10.1147/rd.112.0215

[20] Farhat, C., van der Zee, K. G., Geuzaine, P. "Provably second-order time-accurate loosely-coupled solution algorithms for transient non-linear computational aeroelasticity", Computer Methods in Applied Methods and Engineering, 195(17–18), pp. 1973–2001, 2006.

[21] Scanlan, R. H., Tomko, J. J. "Airfoil and Bridges Deck Flutter Derivatives", Journal of Engineering Mechanics, 97(6), pp. 1717–1737, 1971.

[22] Wu, T., Kareem, A. "Vortex-Induced Vibration of Bridge Decks: Volterra Series-Based Model", Journal of Engineering Mechanics, 139(12), pp. 1831–1843, 2013. https://doi.org/10.1061/(ASCE)EM.1943-7889.0000628

[23] Balajewicz, M., Dowell, E. "Reduced-Order Modeling of Flutter and Limit-Cycle Oscillations Using the Sparse Volterra Series", Journal of Aircraft, 49(6), pp. 1803–1812, 2012. https://doi.org/10.2514/1.C031637

[24] Hübner, B., Walhorn, E., Dinkler, D. "A monolithic approach to fluid-structure interaction using space-time finite elements", Computer Methods in Applied Mechanics and Engineering, 193(23–26), pp. 2087–2104, 2004. https://doi.org/10.1016/j.cma.2004.01.024

[25] Zhang, L. T., Gay, M. "Immersed finite element method for fluid-structure interactions", Journal of Fluids and Structures, 23(6), pp. 839–857, 2007. https://doi.org/10.1016/j.jfluidstructs.2007.01.001

[26] Hockney, R. W. "The potential calculation and some applications", Methods in Computational Physics, 9, pp. 135–211, 1970.

[27] Viré, A., Derksen, A., Folkersma, M., Sarwar, K. "Two-dimensional numerical simulations of vortex-induced vibrations for wind turbine towers", Wind Energy Science, 5, pp 793–806, 2020. https://doi.org/10.5194/wes-5-793-2020

[28] Lu, X., Tian, Y., Sun, C., Zhang, S. "Development and Application of a High-Performance Triangular Shell Element and an Explicit Algorithm in OpenSees for Strongly Nonlinear Analysis", Computer Modeling in Engineering & Science, 120(3), pp. 561–582, 2019. https://doi.org/10.32604/cmes.2019.04770

[29] Ge, Y., Liu, S. "2D Pure-numerical simulation for whole-process wind induced responses of long-span bridge decks", In: 6th International Symposium on Wind Engineering, Hamburg, Germany, 2014, pp. 308–309.

[30] Zhong, J., Xu, Z. "A modal approach for coupled fluid structure computations of wing flutter", Proceedings of the Institution of Mechanical Engineers, Part G: Journal of Aerospace Engineering, 231(1), pp. 72–81, 2016. https://doi.org/10.1177/0954410016644630

[31] Ammann, O. H., Kármán, T., Woodruff, G. B. "The failure of the Tacoma Narrows Bridge", Federal Works Agency, Washington, DC, USA, Rep. 45680, 1941. [online] Available at: https://resolver.caltech.edu/CaltechAUTHORS:20140512-105559175

[32] InterCAD Ltd. "AxisVM" [computer program] Available at: https://axisvm.hu/index.html

[33] Arioli, G., Gazzola, F. "Torsional instability in suspension bridges: The Tacoma Narrows Bridge case", Communications in Nonlinear Science and Numerical Simulation, 42, pp. 342–357, 2017. https://doi.org/10.1016/j.cnsns.2016.05.028

[34] Tuo, C. Z., Bai, Y. G., Sun, D. K., Liu, G., Lin., J. H. "Flutter Derivative Identification using Turbulence Modeling", In: Computation Mechanics, Proceedings of International Symposium on Computational Mechanics, Beijing, China, 2007, pp. 748–757. https://doi.org/10.1007/978-3-540-75999-7_125

[35] Nieto, F., Hargreaves, D. M., Owen, J. S., Hernandez, S. "On the applicability of 2D URANS and SST k-ω turbulence model to the fluid-structure interaction of rectangular cylinders", Engineering Applications of Computational Fluid Mechanics, 9(1), pp. 157–173, 2015. https://doi.org/10.1080/19942060.2015.1004817

[36] Szabó, G. "Tacoma Narrows Bridge Aeroelastic FSI Simulation" [video online] https://www.youtube.com/watch?v=J_Fz1FdXqdk

[37] Stoyanoff, S., Irwin, P. "Flutter Analysis of Lions' Gate Bridge during Deck Replacement", presented at 6th Asia-Pacific Conference on Wind Engineering, Seoul, South Korea, Sept, 12–15, 2005.

[38] Irwin, P. A., Stoyanoff, S., Xie, J., Hunter, M. "Tacoma Narrows 50 years later – wind engineering investigations for parallel bridges", Bridge Structures, 1(1), pp. 3–17, 2005. https://doi.org/10.1080/15732480420002745 51

[39] Ge, Y.-J. "Aerodynamic challenge and limitation in long-span cable-supported bridges", presented at The 2016 World Congress on Advances in Civil, Environmental, and Materials Research (ACEM16), Jeju Island, Korea, Aug, 28–Sept, 1, 2016.

[40] Huang, L., Liao, H., Wang, B., Li, Y. "Numerical simulation for aerodynamic derivatives of bridge deck", Simulation Modelling Practice and Theory, 17(4), pp. 719–729, 2009. https://doi.org/10.1016/j.simpat.2008.12.004

[41] Chawdhury, S., Morgenthal, G. "Numerical simulations of aeroelastic instabilities to optimize the performance of flutter-based electromagnetic energy harvesters", Journal of Intelligent Material Systems and Structures, 29(4), pp. 479–495, 2017. https://doi.org/10.1177/1045389X17711784